Demography of a nearshore gadid (Eleginus nawaga) from the Barents Sea coast during the last glacial period

A. J. Gharrett (✉ a.gharrett@alaska.edu)
  University of Alaska Fairbanks

Natalia V. Chernova
  Zoological Institute of the Russian Academy of Sciences

Noël A. Smé
  University of Alaska Fairbanks

Sarah Lyon
  University of Alaska Fairbanks

Patrick D. Barry
  University of Alaska Fairbanks

Research Article

Additional Declarations: No competing interests reported.

Abstract

Recent glaciations in northwestern Russia completely covered the Barents Sea during four glacial advances. At the peaks of those glacial advances, there were no nearshore macrofauna. Consequently, colonization by species that now inhabit present-day nearshore waters must have occurred since the habitat became available and hospitable, less than 15 ka. We analyzed microsatellite data from *Eleginus nawaga* (Gadiformes: Gadidae) collected from Khaipudyrskaya Bay in the southeastern Barents Sea with coalescent-based models to estimate the times and effective population sizes that existed before and after major historical demographic changes. Colonization of *E. nawaga*, which could only follow establishment of a lower trophic-level food web, provides an indicator of the for that timing. The results of the analyses were consistent with two major demographic events. After an initial founding event from a small number of individuals before ~ 140 ka, the population grew to an effective size of about 2700 individuals. Subsequently, probably as the ice receded after the Last Glacial Maximum, it plateaued at ~ 26,000 about 3000 years ago. Colonization likely came from eastern populations following the Saalian Period, after which there was little nearshore ice to the East of the Kara Sea.

Introduction

Following glacial retreat, some marine habitat loses its ice cover, while other habitat is created by inundation from rising sea level. Newly available habitat is not colonized instantaneously. Organisms at higher trophic levels must await colonization by lower-level prey organisms. Some higher-level species depend on a suite of prey species as they grow from larvae to adults and at different life history stages may seek different prey species in different ecological locations. Consequently, there may be a substantial lag between colonization of lower- and upper-trophic level species. Nevertheless, timing of colonization of upper-level species should indicate when a mature ecosystem with a complex food web has been established.

The genetic composition observed at nearly neutral loci of a species results from processes such as mutation and demographic history. Mutation generates new alleles at a locus and demographic events act stochastically on the abundance of those alleles (e.g. Tajima 1983). In a population at mutation-drift equilibrium, there will be a flux of allelic composition; but the number of allelic states at a locus will remain relatively constant. However, the composition of and relationships between states will vary stochastically, driven by the timing and magnitudes of historic fluctuations in population size. For some kinds of genetic markers, such as microsatellites or DNA sequences and with some simple assumptions, it is possible to estimate genealogies that reflect ancestral compositions and to estimate a demographic history.

In this paper, we examined the establishment of the southwestern Barents Sea nearshore food web from the historical demographics of a small, nearshore gadid, navaga (*Eleginus nawaga*). Only after the recession of glaciers and the rise in sea level began ~ 18 thousand years ago (ka) could nearshore marine organisms colonize Barents Sea habitat. The program Migraine (Leblois et al. 2014) uses coalescence

(e.g. Kingman 2000) to construct likely genealogies for an observed set of alleles at a locus to estimate historic changes in effective population sizes and the times at which the changes occurred. The changes would postdate the establishment of nearshore species at lower trophic levels.

Over the last 100,000 years or so, glaciers have advanced and retreated three times in the northern European and western Russian Arctic (e.g. Svendsen et al. 2004). Each time, ice sheets have merged to create a continuous expanse from the Scandinavian Peninsula to the Taimyr Peninsula (Fig. 1). At the Last Glacial Maximum (LGM) about 20−19 ka (thousand years ago), the ice advance in combination with reduced sea level (Dittmers et al. 2008; Lambeck et al. 2014) completely filled the Barents Sea basin. Consequently, only after the recession of glaciers and the rise in sea level began ~ 18 ka could nearshore marine organisms colonize Barents Sea habitat.

Navaga *Eleginus nawaga*, an arctic bentho-pelagic gadid (Gadiformes: Gadidae) that inhabits estuarine and nearshore waters at shallow (to 40 m) depths and prefers a silty, soft bottom, is abundant in the White, Barents, and Kara seas. Annual migrations are local seasonal movements offshore from the coast and back in the late summer (Maznikova and Orlov 2020). Navaga may have population structure that corresponds to estuaries of rivers that flow into different bays. Genetic structure has also been observed for Pacific herring (*Clupea pallasii*), another nearshore species within the White, Barents, and Kara seas (Semenova et al. 2015).

Life history characteristics of navaga obtained from commercial fisheries on spawning aggregations are consistent with population structure. Differences in relative abundances of age classes and average sizes-at-age have changed during the past 50 years, probably a consequence of increased temperatures and reduction in commercial fishing, which declined when Russia transitioned to a market economy in the mid-1990s (Stasenkov and Goncharov 2020). Data reported for commercial catches (Stasenkov and Goncharov 2020) can be used to estimate average age at reproduction (average generation time) and average size of fish in the catches. In the White, Barents, and Kara seas, average generation times varied from 2.8 to 5.4 years and the weight of individuals averaged 86 to 137 g; in Khaipudyrskaya Bay, the average generation time was 4.5 to 5.0 years and the average size was 86 to 100 g. Prior to the mid-1990s, catches in Khaipudyrskaya Bay averaged 417 mt, which corresponds to between 4.2 and 4.8 million fish, a minimum census size.

Navaga deposit demersal eggs in the winter under ice cover in shallow water from late December to February. Usually, embryogenesis takes place in a narrow temperature range (−2.0 − +2 .0 C) and salinity (not less than 21‰). The duration of egg development is 80−90 days (Makhotin and Novikov 1990). Pelagic juveniles (19−25 mm long) are relatively evenly distributed on the spawning grounds but absent in the open waters of bays (Makhotin and Novikov 1990). The transition of juveniles to the benthic life starts at a length of 25 mm when they move off shore. In July, the length of juveniles is 5−7 cm, in September to December the length of underyearlings is 9−13 cm. By the end of the first year of life (March), juveniles are 12−13 cm long (Makhotin and Novikov 1990). Most of their feeding and growth

takes place when temperatures rise above 0 C, usually between 6 and 12 C. In summer at higher temperatures, they may descend to colder water layers in order to avoid warmer temperatures.

Juveniles feed on zooplankton; as they grow, they switch to feeding on benthic invertebrates, such as polychaetes and crustaceans (amphipods, mysids), as well as small fish. Adult navaga feed on fish (herring, smelt, sand eels, sticklebacks), crustaceans and polychaetes, and also priapulids, fish eggs, molluscs, insect larvae, and seagrass Zostera (Kudersky 1966). Consequently, colonization of the Barents Sea by navaga required flourishing of a mature nearshore ecosystem

Detailing navaga demographic history will provide insight into timelines relative to postglacial colonization events of multiple species in the Barents Sea and nearby waters. Information about that timing may be useful for predicting the spread of colonization following a variety of habitat disruptions. The advantage of the program Migraine is that it can fit several different models that subsume more complex models to make maximum-likelihood estimates of the times and effective sizes of the population when demographic changes occurred in the past. It should be possible to compare results of those models and choose the most appropriate one. Comparing the results of those models with known information about recent glacial history in the Barents Sea (e.g. Mangerud et al. 2004; Svendsen et al. 2004) should provide some insight into the timing of recolonization events. To this end we: (1) obtained microsatellite data from samples of navaga from southeastern Barents Sea population; (2) estimated the timing and population sizes of demographic events resolved with the program Migraine; and (3) interpreted those data in the context of the recent glacial history of the Barents Sea.

Materials And Methods

Collections

Specimens of *E. nawaga* were taken at seven locations off the Varandey coast near Khaipudyrskaya Bay in the southeastern part of the Barents Sea (Fig. 1). This field work was carried out as part of the ecological and fisheries research on board the RV Dalnie Zelentsy (Murmansk Marine Biological Institute of the Kola Scientific Center, Russian Academy of Sciences). The fish collected were captured from 19–24 July 2013, primarily by bottom and Sigsbee trawls, but also by hook and line. Surface temperatures were 12.8–18.3 C and the bottom layer was from – 1.7–2.0 C; surface salinity was 16.5–30.0‰ and the bottom layer was 32.0–33.2‰.

The total number of fish was 88, five collections were small ($n \leq 5$) and two were larger ($n = 27$ and 44). The collections were made less than 65 km from each other (Table 1). Tissue samples were placed in a DNA preservative (Seutin et al. 1991) and sent to the University of Alaska Fairbanks laboratory where they were stored at -20° C. Isolation of DNA and microsatellite amplification and analysis were conducted as described in Smé et al. (2017) for eight tetra-nucleotide microsatellite loci: *Elgr07*, *Elgr11*, *Elgr13*, *Elgr14*, *Elgr23*, *Elgr31*, *Elgr44*, and *Elgr45*.

Analysis

Collections, both individually and combined, were tested for Hardy-Weinberg and linkage equilibrium with GENEPOP ver. 4.5.1 (Rousset 2008). Pseudo-exact tests of homogeneity were made for the set of populations and between pairs of populations with GENEPOP. Significance of multiple tests was corrected with false discovery rates (FDR) (Benjamini and Hochberg 1995).

An estimate of the effective number of breeders (N_b) was made based on linkage disequilibrium with NeEstimator v.2.0 (Do et al. 2014). The extent of relatedness between individuals was estimated with the software package IDENTIX v1.1 (Belkhir et al. 2002); two different estimators, the pairwise relatedness method of moments and maximum likelihood (Lynch and Ritland 1999) and Identity (Mathieu et al. 1990), were used. A test for a recent (0.2 – 4.0 N_e generations) bottleneck was made with the program Bottleneck (Piry et al. 1999). The mutational model used for the tetra-nucleotide microsatellite loci was the stepwise-mutation model (SMM) (Sun 2012). Significantly small heterozygosities, those expected under Hardy-Weinberg proportions compared to expectations under drift-mutation equilibrium for the observed number of alleles, are consistent with an expanding population (Cornuet and Luikart 1996).

Migraine (Leblois et al. 2014) uses coalescence to simulate phylogenetic trees from microsatellite data and to estimate parameters for the times in the past and the effective population sizes of demographic events. The program offers two models for data from single populations: (1) OnePopVarSize models a single past change in population size and (2) OnePopFounderFlush models two past changes in population size. In two parameterizations of the OnePopVarSize model there is a change (increase or decrease) from the ancestral size (N_{anc}) D generations in the past to the size of the sampled population, or to T generations before the present since when it has remained constant. Estimates of the general parameters are scaled by mutation rate (μ) because estimates of N_e are confounded with μ: $2N\mu$, $2N_{anc}\mu$, $D/2N$, and $T/2N$, for which the Ns are the number of alleles – twice the diploid number of individuals; note that $2N\mu$ is Θ, the generalized Watterson (1975) estimator. The program can also estimate standardized numbers of $D\mu$ and $T\mu$, so that the effective population sizes and number of generations before present can be estimated if mutation rates are known. Migraine makes iterative maximum-likelihood estimates of demographic parameters of effective population sizes and times of events in the past from phylogenies simulated by coalescence. Because the analysis is computer intensive, we used the Regional Computing System at the University of Alaska (UAF). Custom BASH (Bourne again shell) scripts for the SLURM (Simple Linux Utility for Resource Management) managed cluster at UAF were written (Online Resource 2). OnePopFounderFlush considers two past changes in effective population size that began from the ancestral size (N_{anc}), which changed to a founder population effective size (N_{found}) D generations ago and then expanded (or contracted) to the present size (N) or to a time, T generations before present, after which the effective population size was stable. The conditions for the analyses include: the number of trees that are constructed and evaluated at each iteration; the number of iterations for the analysis; and whether results of an iteration, selected by their likelihoods, are written over or appended to results of the previous iteration (Rousset et al 2018).

Some of the demographic parameters estimated in preliminary analyses with Migraine appeared not to converge or had large confidence intervals; examples are in Online Resource 1 Figs. 2, 3, and 4. The reasons for these kinds of results could be the specification of too few trees for each iteration, making too few iterations, having an insufficient number of microsatellite loci, or testing the wrong model. We explored these possibilities by: (1) specifying either 2000 or 50,000 trees in each iteration; (2) increasing the number of iterations that overwrote previous results; and (3) by artificially doubling the number of loci. The last approach does not produce estimates that could be used to describe the demographic history; but because the loci are evaluated independently in the program, the results can provide insight on the effect of increasing the number of loci.

Results

Microsatellite data for eight loci were obtained for the 88 individuals from 7 collections (Online Resource 3). No test of the data indicated a departure from Hardy-Weinberg or linkage equilibrium; of course, only tests of the two larger collections and combination of collections were meaningful. Departures from homogeneity were not detected. Subsequently, all analyses were conducted on the combined data.

The estimate for N_b that used all alleles was 694.2 (95% parametric CI: 355.7−6790.5). The upper limit for estimates when rare alleles were omitted was infinite, which is consistent with the small sample size. Navaga does not have discrete generations, so an estimate of N_e would reflect the effective number of breeders of the cohorts. For an average generation time of 5 years, an estimate of N_e would be between about 1778 and 33,952 individuals.

None of the estimates for relatedness from IDENTIX v1.1 or their variances were significant ($P > 0.10$). All three of the tests for bottlenecks (sign test, standardized test, and Wilcoxon test) were significantly small ($P < 0.05$) for the SMM.

Results of Migraine analyses with variation in tree numbers and iterations indicated that the OnePopFounderFlush model that included a current population size that had been stable for T generations provided the best fit to the microsatellite data (Online Resource 1).

Those results were consistent with a present-day effective population of about 26,000 diploid individuals (assumed mutation rate of 10^{-3}; Sun 2012) that has been stable for about 3000 years (Table 2), a number that had climbed from an ancestral size near zero, although the confidence interval was enormous (Table 2 and Fig. 2) since about 143,000 years before present, an estimate that also had a large confidence interval (Table 2 and plots in Online Resource 2 Fig. 12). Those results suggest that the population was founded by a very small number of individuals within the last 100,000 or so years. That number expanded to the current effective size about 3000 years ago and has been stable since.

Discussion

The Migraine model most consistent with our data included two demographic changes, a change from an ancestral effective population size (N_{anc}) followed by an increase to a founder size (N_{found}) until recently when the size stabilized at the present-day effective size (N). To interpret these sizes and times in the past, we will briefly review glacial history of the Barents Sea and nearby regions. Marine isotope stage (MIS) corresponds to a temporal index based on the ratio of the ^{16}O and ^{18}O isotopes in deep-sea core sediments; relatively higher levels of ^{18}O reflect colder periods (e.g. Urey et al. 1951). From ~ 190−140 ka (MIS 6), the Late Saalian Glacial stage advanced far into northern Europe and western Russia (Hughes and Gibbard 2018), well past the limits of the Last Glacial Maximum (LGM) ~ 20−19 ka during the Late Weichselian (MIS 2; 25−15 ka) (Svendsen et al. 2004). There is evidence that much of the land-locked Arctic Ocean was covered with an ice sheet at MIS 6 (~ 140 ka) and high points on the ocean floor probably pinned the > 1000 m thick sheet (Jakobsson et al. 2016). This means that there would have been little macrofauna at that time in the western Arctic Ocean and colonization of species like navaga must have occurred subsequently.

Following the Late Saalian period was an interglacial, the Eemian period (MIS 5e; ~130−115 ka), which may have been warmer than our present climate (Sakari Salonen et al. 2018). Next came the Weichselian period, during which glaciers advanced three times: (1) the Early Weichselian (100−80 ka; MIS 5d), (2) the Middle Weichselian (60−50 ka; MIS 3) and (3) the Late Weichselian (25−15 ka; MIS 2). Each was followed by deglaciation (Svendsen et al. 2004). The Early Weichselian glaciation was the most extensive; the Kara, Barents, and Scandinavian ice sheets coalesced to extend from the Scandinavian Peninsula to the Taymyr Peninsula, which is the western boundary of the Laptev Sea. Grounded ice completely covered the Barents and Kara Seas from the coastline to the continental shelf. Inside the Russian ice sheet, large proglacial lakes formed, which probably drained through the Volga River to the Aral Sea (Soulet et al. 2013). When the glaciers receded, an enormous volume of water erupted through the southern Barents Sea and through the Baltic Sea (Mangerud et al. 2004). A combination of the grounded ice and huge water flow through the shallow coastal waters precludes the existence of navaga at our sampling sites during this period. During the Middle Weichselian, grounded ice sheets again were continuous from the Scandinavian Peninsula to the Taymyr Peninsula and proglacial lakes formed south of the Russian glaciers. At the end of this period, the proglacial lake waters probably flowed north. During the Late Weichselian, coalesced ice sheets extended through the Barents and Kara seas, but there appeared to be only peripheral proglacial lake formation (Mangerud et al. 2004). The regional ice volumes varied during the three Weichselian glaciations. Ice was thickest in the east during the Early Weichselian; whereas, there was more extensive glaciation from the Scandinavian Ice sheet during the Late Weichselian (Svendsen et al. 2004). Nevertheless, there is evidence of grounded ice throughout the Barents Sea (Landvik et al. 1998) during all three periods.

The demographic estimates from the microsatellite data can be interpreted in terms of the glacial history. During the Eemian interglacial, which followed the Late Saalian when much of the Arctic Ocean was ice covered, nearshore habitat became available. Our analysis detected a first demographic event that was ~ 140 ka, which is consistent with the Eemian interglacial. The effective population size at that time was

about 2700 individuals. The ancestral population preceding that time was much smaller than that of the present day (Fig. 2, Table 2). The results of the model we applied in Migraine indicated that the current population size (about 26,000) had been attained by the time of the second demographic event. That means that the population had expanded about 10-fold since the Eemian. Constrained by the models available in Migraine, the population growth was modeled assuming exponential growth. However, it is unlikely continuous growth occurred because appropriate habitat did not become instantaneously available, rather it probably expanded slowly. Habitat in the Barents Sea was unavailable until ice retreated starting ~ 15 ka and the southern connection between the Barents and Kara seas was not available until ~ 10 ka (Fig. 3). Also, most of the rise in sea level was not complete until ~ 7 ka (Lambeck et al. 2014). It would be expected that habitat did not actually become available to navaga until the ecosystem expanded to include an appropriate complex of prey populations, which would lag behind simple access to the shallow nearshore marine environment. From the known present-day distribution, it seems likely that the colonization occurred as a westward movement from the Laptev or East Siberian seas. Because the western Russian Arctic coast was not continually ice-covered during the Weichselian advances, that area may have been a refugium. The estimate of the present-day effective population size from the coalescent model of Migraine was ~ 26,000, which was included in the range (1778–33,952) estimated from the linkage disequilibrium method. In contrast, the census size exceeds 4 million fish. The estimate from Migraine makes use of the distribution and suite of alleles to construct an historic estimate; whereas, NeEstimator looks at the linkage disequilibrium for pairs of alleles, but does not use the information provided by the sizes of the alleles. Regardless, the census size far exceeds effective numbers, possibly as a consequence of the recent colonization compounded by large variance in family size and inter-annual variation in the number of recruits.

Our last question is the source of the colonization of navaga following the LGM. Nucleotide sequence data from the mitochondrial cytochrome B gene of navaga and its sister taxon, saffron cod (*E. gracilis*), suggest that they diverged ~ 2.32 Ma (million years ago), as did several other vicariant species pairs (Laakkonen et al. 2021). The Pliocene cooling that took place 3.5–3.1 Ma (e.g. De Schepper et al 2015) was followed by a large glacial advance between ~ 3.6 and 2.4 Ma (Matthiessen et al 2009), after which cooling, relative to the earlier Pliocene and Miocene, continued through the Pleistocene to the present. Prior to complete closure of the Isthmus of Panama, the connection between the Pacific and Atlantic oceans had a depth of at least 1200 m (O'Dea et al. 2016). Subsequently, global oceanic current patterns were radically altered (e.g. De Schepper et al. 2015). One of the consequences of the changes in oceanic currents was the reversal of flow through the Arctic from the Pacific Ocean to the Atlantic Ocean during interglacial periods, when the water level was high enough to inundate the Bering Strait (e.g. De Schepper et al. 2015).

The mitochondrial nucleotide sequence data suggest that there was no contact between navaga and saffron cod subsequent to their divergence (Laakkonen et al. 2015). Biogeographical patterns deduced from mitochondrial gene sequences suggest that 34 taxa, which include mollusks, crustaceans, and fish also have a deep vicariance between the Pacific and Atlantic oceans (Laakkonen et al. 2015). Although *E.*

nawaga and *E. gracilis* have slightly diverged morphologically; they can be difficult to distinguish without close scrutiny that may include dissection (Vasil'eva 1997).

During the Pleistocene, multiple glacial advances blocked access through the Bering Strait (Miller et al. 2020). As in the Late Pleistocene (the Saalian and Weichselian glacial cycles), the Arctic Ocean of northern Europe and northwestern Russia was completely covered by glaciers, as was the coastline of Greenland and North America. The Arctic coastal areas of eastern Siberia, which included much of the large continental shelf, were not glaciated (e.g. Batchelor et al. 2019), but were probably covered by seasonal ice. The resulting large coastal plain was grasslands, which supported grazers such as wooly mammoths and horses (Sher et al. 2005). Also during the late Pliocene and early Pleistocene, because of uplift in eastern Asia, Siberian rivers (Lena, Ob, and Yenisey) began to drain into the Arctic Ocean (e.g. Ma et al. 2021). Those rivers now contribute much of the total freshwater flow into the Arctic Ocean. The estuaries that were created could have served as favorable navaga habitat. It seems likely that the Laptev and Eastern Siberian seas may have provided refuge for navaga during glacial advances that occurred subsequent to the separation of navaga and saffron cod lineages.

What do we know about the ranges of navaga and saffron cod at present? There appears to be a several thousand kilometer disjunction, from the western Laptev Sea to the Chukchi Sea. The documented eastern limit for navaga is the Khatanga Bay in the western Laptev Sea (Ulchenko et al. 2016). Records of more eastern navaga are erroneous or undocumented. The most cited original report (Borisov 1928) of navaga for the Laptev Sea (the Lena River delta) was a misidentification of an *Arctogadus borisovi* specimen (Svetovidov 1948). There are no recent records of navaga in field studies in the Lena drainage, the Lena Polynya, the Laptev Sea shelf, or in the East-Siberian Sea (Gukov 1999; Chernova 2015; Orlov et al. 2020a, b).

The western limit of saffron cod is Kolyuchinskaya Bay in the western Chukchi Sea (Rendahl 1931). Saffron cod were not listed for Chaunskaya Bay in the western East Siberian Sea (Neelov 2008; Chernova 2022) nor caught in trawl surveys on shelf of the East Siberian Sea (e.g. Glebov et al. 2016; Orlov et al. 2020c). Although saffron cod are included in a few compilations of fish species of the East Siberian and Laptev seas), there is no documentation. Thus, at present navaga and saffron cod seem to be absent in the area between the Khatanga Bay (western Laptev Sea) and Kolyuchinskaya Bay (western Chukchi Sea).

In the coastal areas of the Siberian Arctic, the modern climate is colder than it was in the late Pleistocene – early Holocene. This process is well documented by the succession of paleoflora (Svitoch 1980). During the climate optimum, the coastal region was occupied by forest and shrub tundra with thickets of birch, alder, and dwarf forests. As a result of a climate cooling that started 5–4 ka, this vegetation was replaced by arctic-type tundra. Paleoichthyology provides similar evidence. Fossil remains of freshwater fish were identified in sediments (~ 12 ka) in the region of Chaunskaya Bay (Nazarkin 1992). Several species (e.g. Crucian carp *Carassius* sp., lake minnow *Phoxinus percnurus* (= *Rhynchocypris percnura*),

longnose sucker *Catostomus catostomus*, and European perch *Perca fluviatilis*) no longer inhabit the area, presumably because of Holocene cooling (Nazarkin 1992).

Perhaps Holocene climate cooling explains the modern absence of the navaga and saffron cod in the coastal Siberian water. The Laptev and East Siberian seas are among the harshest Arctic areas. The duration of the ice-free period ranges from 1−1.5 months in the northeast to 2.5−3 months in the southeast. The greatest influx of solar radiation falls on May-June, when the sea is still covered with ice and 60% of the incoming radiation reflects into the atmosphere (Ecological Atlas 2017). Warm currents of neither the Pacific nor Atlantic oceans penetrate into Siberian shelf areas (Anderson and Macdonald 2015). Although water temperatures have increased during the last 20 years (Golubeva et al. 2021), the East Siberia shelf is still less saline (< 20‰) and colder (1−5 C) in the summer than the Kara, Barents, and White sea coasts and freshwater intrudes down to ~ 25 m along much of the coast. The enormous rivers also deliver substantial amounts of clay and silt, which characterize the very broad shelf of the East Siberian Sea (e.g. Kokarev et al. 2021). The result of the physical environment is an ecosystem with low productivity. All these factors make habitat unfavorable for both navaga and saffron cod. This cold Siberian "spot" may limit the distribution of saffron cod from the Pacific along the Asian coast. It also may have caused the disappearance of navaga from this area. Navaga may have been distributed more widely during the boreal optimum, eastward of the Kara-Barents seas, but after the Holocene cooling, it could have been concentrated along the western Siberian coast; the modern range of navaga may be a recent refuge.

Declarations

Author contribution.

AJG conceived the project, conducted much of the analysis drafted the manuscript. NVC provided the samples and contributed to the writing. NAS and SL conducted the laboratory analysis and contributed to the analysis. PDB contributed to the Migraine analysis and writing.

Data Archiving

Data are tabled in Online Resource 3.

Ethical approval

All applicable national and international guidelines for the care and use of animals were followed.

Conflict of Interest

The authors declare no competing interests.

Acknowledgements

References

1. Amante C, Eakins BW (2009) ETOP1 1 Arc-minute global relief model: procedures, data sources, and analysis. NOAA Tech Memo NMFS NESDIS NGDC-24. 10.7289/V5C8276M. Accessed 7 Nov 2017

2. Anderson LG, Macdonald RW (2015) Observing the Arctic Ocean carbon cycle in a changing environment. Polar Res 34:26891. https://dx.doi.org/10.3402/polar.v34.26891

3. Batchelor CL, Margold M, Krapp M, Murton DK, Dalton AS, Gibbard PL, Stokes CR, Murton JB, Manica A (2019) The configuration of Northern Hemisphere ice sheets through the Quaternary. Nat Commun 10:3713. https://doi.org/10.1038/s41467-019-11601-2

4. Belkhir K, Castric V, Bonhomme F (2002) IDENTIX, a software to test for relatedness in a population using permutation methods. Mol Ecol Notes 2:611–614. https://doi.org/10.1046/j.1471-8278.2002.00273.x

5. Benjamini Y, Hochberg Y (1995) Controlling the false discovery rate: a practical and powerful approach to multiple testing. J R Stat S B 57:289–300. https://doi.org/10.1111/j.2517-6161.1995.tb02031.x

6. Borisov PG (1928) Dog-salmon (keta) and navaga from the basin of the River Lena. Materials of the Commission for the Study of the Yakut Autonomous Soviet Socialist Republic. Leningrad 27:1–26. (In Russian)

7. Chernova NV (2015) Marine fishes of the New-Siberian Islands (protected zone of the Ust-Lensky Reserve). Scientific papers of the Prisursky State natural reserve. 30(1):271–276 (In Russian).

8. Chernova NV (2022) Overview of the fish fauna of the Chaunskaya basin – the area of the natural reserve "Chaunskaya Guba" and the port of Pevek (East Siberian Arctic). Proceedings of the Zoological Institute RAS, 326(1):30–42. (In Russian) https://doi.org/10.31610/trudyzin/2022.326.1.30

9. Cornuet JM, Luikart G (1996) Description and power analysis of two tests for detecting recent population bottlenecks from allele frequency data. Genetics 144:2001–2014.

10. https://doi.org/10.1093/genetics/144.4.2001

11. De Schepper S, Schreck M, Beck KM, Matthiessen J, Fahl K, Mangerud G (2015) Early Pliocene onset of modern Nordic Sea circulation related to ocean gateway changes. Nat Commun 6:8659.

https://doi.org/10.1038/ncomms9659

12. Dittmers K, Niessen F, Stein R (2008) Acoustic facies on the inner Kara Sea Shelf: Implications for Late Weichselian to Holocene sediment dynamics. Mar Geol 245:197–215. https://doi.org/10.1016/j.margeo.2008.06.004

13. Do C, Waples RS, Teel D, Macbeth GM, Tillett BJ, Ovenden JR (2014) NeEstimator V2: re-implementation of software for the estimation of contemporary effective population size (*Ne*) from genetic data. Mol Ecol Res 14:209–214. https://doi.org/10.1111/1755-0998.12157

14. Ecological Atlas. Laptev Sea (2017) Moscow, Arctic Scientific Center, 303 pp (In Russian).

15. ESRI (Environmental Systems Research Institute) (2011) ArcGIS Desktop: Release 10.1. Environmental Systems Research Institute, Redlands.

16. Glebov II, Nadtochiy VA, Savin AB, Slabinsky AM, Borilko OYu, Chulchekov DN, Sokolov, AS (2016) Results of comprehensive research in the East-Siberian Sea in August 2015. Izvestiya TINRO 186:8–92. (In Russian). https://doi.org/10.26428/1606-9919-2016-186-81-92

17. Golubeva E, Kraineva M, Platov G, Iakshina D, Tarkhanova M (2021) Marine heatwaves in Siberian Arctic seas and adjacent region. Remote Sens 13:4436. https://doi.org/10.3390/rs13214436

18. Gukov AYu (1999) Ecosystem of the Siberian Polynya. Scientific World, Moscow, Russia 334 p (In Russian).

19. Hughes PD, Gibbard PL (2018) Global glacier dynamics during 100 ka Pleistocene glacial cycles. Quatern Res 90:222–243. https://doi.org/10.1017/qua.2018.37

20. Hughes ALC, Gyllencreutz R, Lohne ØS, Mangerud J, Svendsen JJ (2016) The last Eurasian ice sheets – a chronological database and time-slice reconstruction, DATED-1. Boreas 45:1–45. https://doi.org/0.1111/bor.12142

21. Jakobsson M, Nilsson J, Anderson L, Backman J, Björk G, Cronin TM, Kirchner N, Koshurnikov A, Mayer L, Noormets R, O'Regan M, Stranne C, Ananiev R, Barrientos Macho N, Cherniykh D, Coxall H, Eriksson B, Flodén T, Gemery L, Gustafsson Ö, Jerram K, Johansson C, Khortov A, Mohammad R, Semiletov I (2016) Evidence for an ice shelf covering the central Arctic Ocean during the penultimate glaciation. Nat Commun 7:1–10. https://doi.org/10.1038/ncomms10365

22. Kingman JFC (2000) Origins of the coalescent: 1974–1982. Genetics 156:1461–1463. https://doi.org/10.1093/genetics/156.4.1461

23. Kokarev VN, Vedenin AA, Polukhin AA, Basin AB (2021) Taxonomic and functional patterns of macrobenthic communities on a high Arctic shelf: A case study from the East Siberian Sea. J Sea Res 174:102078. https://doi.org/10.1016/j.seares.2021.102078

24. Kudersky LA (1966) Changes in the diet of the White Sea navaga depending on its size in connection with intraspecific food relationships. Voprosy Ikhtiologii 6(2):346–351. (In Russian)

25. Laakkonen HM, Hardman M, Strelkov P, Väinölä R (2021) Cycles of trans-Arctic dispersal and vicariance, and diversification of the amphi-boreal marine fauna. J Evol Biol 34:73–96. https://doi.org/10.1111/jeb.13674

26. Lambeck K, Rouby H, Purcella A, Sun Y, Sambridge M (2014) Sea level and global ice volumes from the Last Glacial Maximum to the Holocene. Proc Nat Acad Sci USA 111:5296–15303. https://doi.org/10.1073/pnas.14117 62111

27. Landvik JY, Bondevik S, Elverøi A, Fjeldskaar W, Mangerud J, Salvigsen O, Siegert MJ, Svendsen J-li, Vorren TO (1998) The Last Glacial Maximum of Svalbard and the Barents Sea area: Ice sheet extent and configuration. Quatern Sci Rev 17:43–75. https://doi.org/10.1016/S0277-3791(97)00066-8

28. Leblois R, Pudlo P, Néron J, Bertaux F, Beeravolu CR, Vitalis R, Rousset F (2014) Maximum-likelihood inference of population size contractions from microsatellite data. Mol Biol Evol 31(10):2805–2823. https://doi.org/10.1093/molbev/msu212

29. Lynch M, Ritland K (1999) Estimation of pairwise relatedness with molecular markers. Genetics 152:1753–1766. https://doi.org/10.1093/genetics/152.4.1753

30. Ma Y, Zheng D, Zhang H, Pang P, Wang W, Wang Y, Wu Y, He H, Stuart FM, Xu S (2021) Plio-Pleistocene establishment of Irtysh River in Junggar, Northwest China: Implications for Siberian-Arctic river system evolution and resulting climate impact. Geophys Res Lett 48:e2021GL093217. https://doi.org/10.1029/2021GL093217

31. Mangerud J, Jakobsson M, Alexanderson H, Astakhov V, Clarke GKC, Henriksen M, Hjort C, Krinner G, Lunkka J-P, Möller P, Murray A, Nikolskaya O, Saarnisto M, Svendsen JI (2004) Ice-dammed lakes and rerouting of the drainage of northern Eurasia during the Last Glaciation. Quatern Sci Rev 23:1313–1332. https://doi.org/10.1016/j.quascirev.2003.12.009

32. Makhotin VV, Novikov GG (1990) Features of the biology of the White Sea cod fish in early ontogenesis. Problems of the study, rational use and protection of natural resources of the White Sea. Abstracts. Materials of the IV regional conference. Arkhangelsk, Zoological Institute of the Russian Academy of Sciences. pp 268–271.

33. Mathieu E, Autem M, Roux M, Bonhomme F (1990) Épreuves devalidation dans l'analyse de structures génétiques multivariées:comment tester l'équilibre panmictique? Rev Stat Appl 38:47–66. http://www.numdam.org/item/RSA_1990__38_1_47_0/

34. Matthiessen J, Knies J, Vogt C, Stein R (2009) Pliocene palaeoceanography of the Arctic Ocean and subarctic seas. Philos Trans Royal Soc A 367:21–48. https://doi.org/10.1098/rsta.2008.0203

35. Maznikova OA, Orlov AM (2020) Navaga *Eleginus nawaga* of the White Sea: a brief review with emphasis on the SovietRussian literature. Polar Biol 43:1159–1173. https://doi.org/10.1007/s00300-020-02681-8

36. Miller KG, Browning JV, Schmelz WJ, Kopp RE, Mountain GS, Wright JD (2020). Cenozoic sea-level and cryospheric evolution from deep-sea geochemical and continental margin records. Sci Adv 6(20):eaaz1346. https://doi.org/10.1126/sciadv.aaz1346

37. Nazarkin MV (1992) Freshwater fish from Late Quaternary sediments of the coast of the East Siberian Sea. Voprosy Ichthyologii 32(5):48–6. (In Russian).

38. Neelov AV (2008) Fish of the Chaunskaya Bay of the East Siberian Sea. Arctic and Antarctic 6(40):154–184. (In Russian).

39. O'Dea A, Lessios HA, Coates AG, Eytan RI, Restrepo-Moreno SA, Cione AL, Collins LS, de Queiroz A, Farris DW, Norris RD, Stallard FF, Woodburne MO, Aguilera O, Aubry M-P, Berggren WA, Budd AF, Cozzuol MA, Coppard SE, Duque-Caro H, Finnegan S, Gasparini GM, Grossman EL, Johnson LG, Keigwin LD, Knowlton N, Leigh EG, Leonard-Pingel JS, Marko PB, Pyenson ND, Rachello-Dolmen PG, Soibelzon E, Soibelzon L, Todd JA, Vermeij GJ, Jackson JBC (2016) Formation of the Isthmus of Panama. Sci Adv 2(8):e1600883. https://doi.org/10.1126/sciadv.1600883

40. Orlov AM, Benzik AN, Vedishcheva EV, Gorbatenko K M, Goryanina SV, Zubarevich VL, Kodryan KV, Nosov MA, Orlova SYu, Pedchenko AP, Rybakov MO, Sokolov AM (2020a) Preliminary results of fishery research in the Laptev Sea onboard the R/V Professor Levanidov in September 2019. Proceedings of VNIRO 179:206–225 (In Russian). https://doi.org/10.36038/2307-3497-2020-179-206-225

41. Orlov AM, Benzik AN, Vedischeva EV, Gorbatenko KM, Goryanina SV, Zubarevich VL, Kodryan,KV, Nosov M A, Orlova SYu, Pedchenko AP, Rybakov MO, Sokolov AM (2020c). Preliminary results of fishery research in the East Siberian Sea on the R/V Professor Levanidov in September 2019. Proceedings of VNIRO 179:187–205. (In Russian). https://doi.org/10.36038/2307-3497-2020-179-187-205

42. Orlov AM, Savin AB, Gorbatenko KM, Benzik AN, Morozov TB, Rybakov MO, Terent'ev DA, Vedishcheva EV, Kurbanov YuK, Nosov MA, Orlova SYu (2020b) Biological research in the Russian Far Eastern and Arctic seas during the VNIRO transarctic expedition. Proceedings of VNIRO 181:102–143. (In Russian). https://doi.org/10.36038/2307-3497-2020-181-102-143

43. Piry S, Luikart G, Cornuet JM (1999) BOTTLENECK: A computer program for detecting recent reductions in the effective population size using allele frequency data. J Hered 90(4):502–503. https://doi.org/10.1093/jhered/90.4.502

44. Rendahl H (1931). Fishe aus dem östlichen Sibirischen Eismeer und dem Nordpazifik. Arkiv för Zoologi 22A(10):1–81.

45. Rousset F, Beeravolu CR, Leblois R (2018) Likelihood computation and inference of demographic and mutational parameters from population genetic data under coalescent approximations. J Soc Fr Statistique **159(3)**:142–166.

46. Rousset F (2008) GENEPOP'007: a complete re-implementation software for Windows and Linux. Mol Ecol Res 8:103–106. https://doi.org/10.1111/j.1471-8286.2007.01931 .x

47. Sakari Salonen J, Helmens KF, Brendryen J, Kuosmanen N, Väliranta M, Goring S, Korpela M, Kylander M, Philip A, Plikk A, Renssen H, Luoto M (2018) Abrupt high-latitude climate events and decoupled seasonal trends during the Eemian. Nat Commun 9:2851. https://doi.org:10.1038/s41467-018-05314-1

48. Semenova AV, Stroganov AN, Afanasiev KI, Rubtsova GA (2015) Population structure and variability of Pacific herring (*Clupea pallasii*) in the White Sea, Barents and Kara Seas revealed by microsatellite DNA analyses. Polar Biol 38:951–965. https://doi.com/10.1007/s00300-015-1653-8

49. Seutin G, White NN, Boag PT (1991) Preservation of avian blood and tissue samples for DNA analysis. Can J Zool 69:82–90. https://doi.org/10.1139/z91-013

50. Sher AV, Kuzmina SA, Kuznetsova TV, Sulerzhitsky LD (2005) New insights into the Weichselian environment and climate of the East Siberian Arctic, derived from fossil insects, plants, and mammals. Quatern Sci Rev 24:533–569. https://do.org/10.1016/j.quascirev.2004.09.007

51. Smé N, Lyon S, Canino M, Chernova N, O'Bryhim J, Lance S, Jones K, Mueter F, Gharrett A (2017) Distinction of saffron cod (*Eleginus gracilis*) from several other gadid species by using microsatellite markers. Fish Bull 116(1) 60–68. https://doi.org/10.7755/FB.116.1.6

52. Soulet G, Ménot G, Bayon G, Rostek F, Ponzevera E, Toucanne S, Lericolais G, Bard E (2013) Abrupt drainage cycles of the Fennoscandian Ice Sheet. Proc Nat Acad Sci USA 110(17):6682–6687. https://doi.org/10.1073/pnas.1214676110

53. Stasenkov VA, Goncharov YuA (2020) Size and age structure of navaga *Eleginus nawaga* of the White, Barents and Kara seas. J Ichthyol 60(3):297–308. https://doi.org/10.1007/s00300-020-02681-8

54. Sun JX, Helgason A, Masson G, Ebenesersdóttir SS, Li H, Mallick S, Gnerre A, Patterson N, Kong A, Reich D, Stefansson K (2012) A direct characterization of human mutation based on microsatellites. Nat Genet 44(10):1161–1165. https://doi:10.1038/ng.2398

55. Svendsen JI, Alexanderson H, Astakhov VI, Demidov I, Dowdeswell JA, Funder S, Gataulling V, Henriksen M, Hjort C, Houmark-Nielsen M, Hubberten HW, Ingólfsson Ó, Jakobsson M, Kjær KH, Larsen E, Lokrantz H, Lunkka JP, Lyså A, Mangerud J, Matiouchkov A, Murray A, Möller P, Niessen F, Nikolskaya O, Polyak L, Saarnistou M, Siegert C, Siegert MJ, Spielhagen RF, Stein R (2004) Late Quaternary ice sheet history of northern Eurasia. Quat Sci Rev 23:1229–1271. https://doi.org/10.1016/j.quascirev.2003.12.008

56. Svetovidov AM (1948) Gadiformes. In Fauna of USSR, Vo IX No. 4. Fishes. Zoological. Institute of the academy of Sciences of the USSR (Translated by the Israel Program for for the National Science Foundation and Smithsonian Institution as OTS 63–11071).

57. Svitoch AA (1980) Paleogeography of the region in the Neogene-Pleistocene. Recent deposits and paleogeography of the Pleistocene of Chukotka. Moscow, Science: 236–243. (In Russian).

58. Tajima F (1983) Evolutionary relationship of DNA sequences in finite populations. Genetics 105:437–460. https://doi.org/10.1093/genetics/105.2.437

59. Ulchenko VA, Matkovsky AK, Stepanov SI, Kochetkov PA, Yankova NV, Gadinov AN (2016) Fish resources and their development in the estuaries of the Kara Sea and the Laptev Sea. Trudy VNIRO 160:116–132. (In Russian)

60. Urey HC, Lowenstam HA, Epstein S, McKinney CR (1951) Measurement of paleotemperatures and temperatures of the upper cretaceous of England, Denmark, and the southeastern United States. Geol Soc Am Bull 62:399–416. https://doi.org/10.1007/s12594-014-0006-5

61. Vasil'eva ED (1997) Morphological divergence of two species of gadid fishes *Eleginus navaga* and *E. gracilis* (Gadidae), with disjunctive area. Voprosy Ikhtiologii 37(6):791–797, (In Russian)

62. Watterson GA (1975) On the number of segregating sites in genetical models without recombination. Theor Popul Biol 7(2):256–276. doi: 10.1016/0040-5809(75)90020-9

Tables

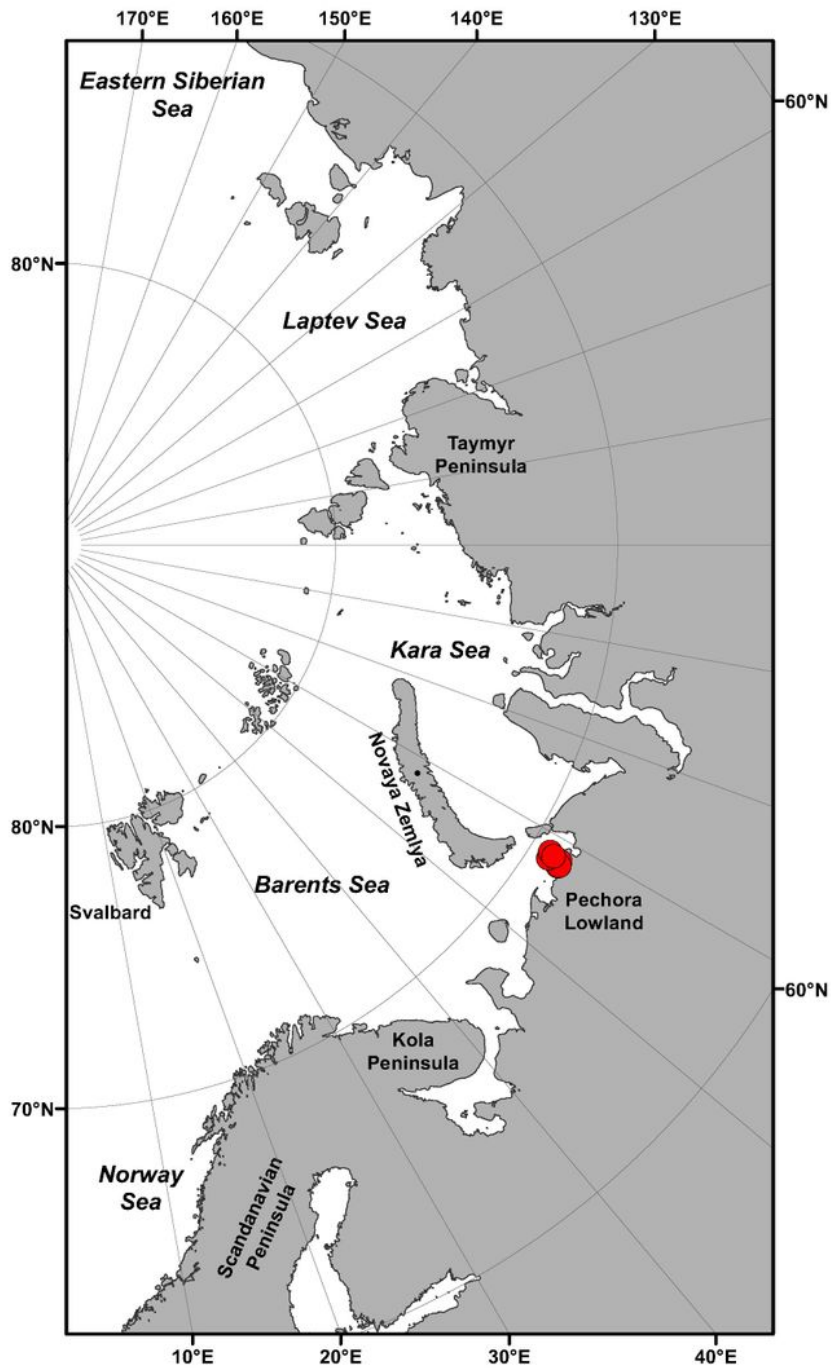Table 1 and 2 are available in the Supplemental Files section.

Figures

Figure 1

Map of the northwest Russian and northern European Arctic coast. The circles just above the label for Pechora Lowlands are the locations from which samples of navaga were collected (see Table 1). The map was constructed in ArcView (ESRI 2011) from ETOPO1 1 arc-minute data (Amante and Eakins 2009).
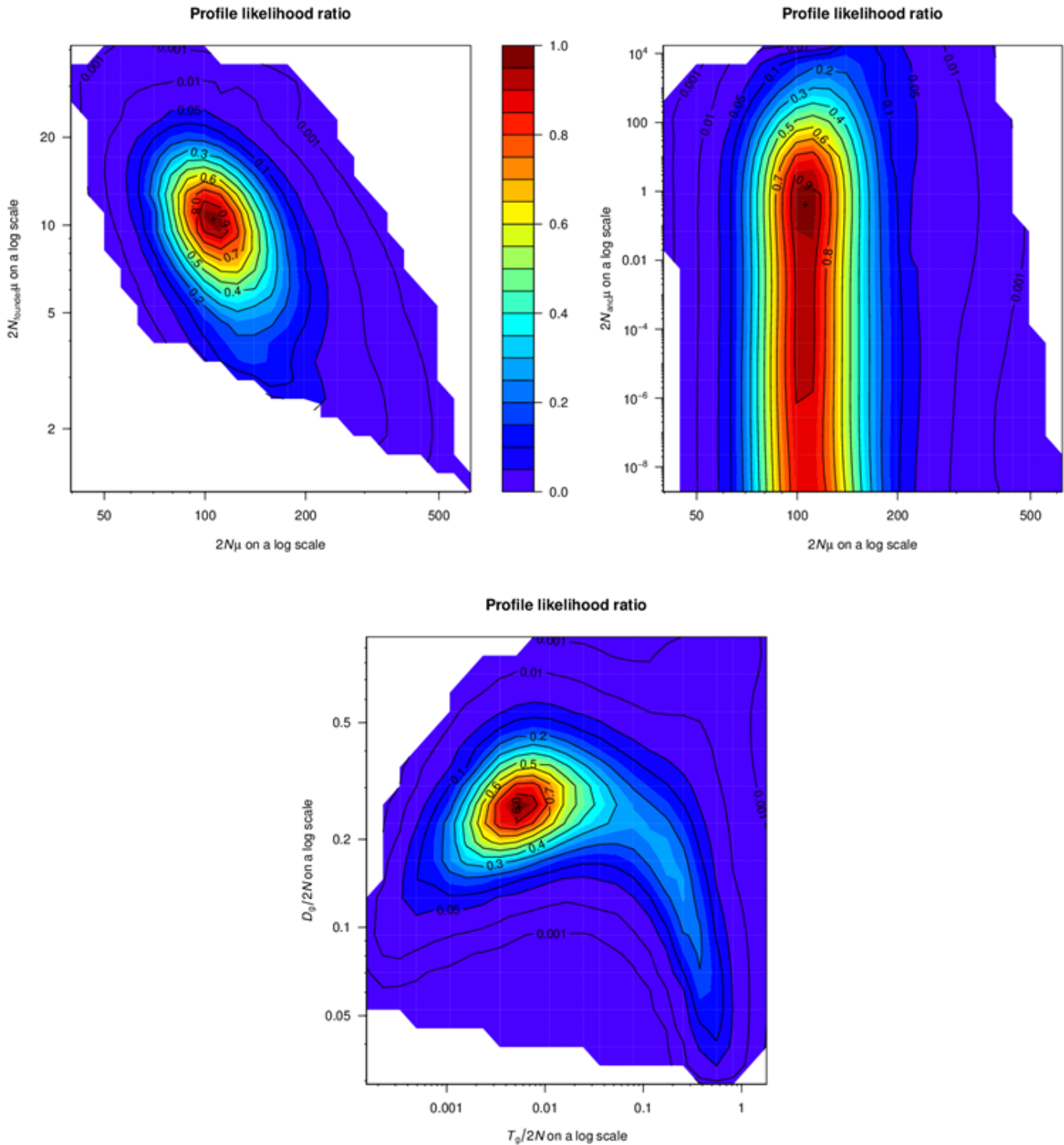
Figure 2

Pairwise likelihood-ratio profiles obtained with Migraine (Leblois et al. 2014) for population sizes and times of population changes for the OnePopFounderFlush model for which *T* was estimated for Barents Sea *E. nawaga* data. Migraine was conducted with 12 iterations in which the previous points were overwritten by the points estimated from the likelihood space of the previous iteration. For the final four iterations, the data points were appended to the points of the previous iteration. Each iteration used

50,000 trees. The vertical bar shows color codes for the chi-square probabilities of the likelihood ratios for parameter pairs relative to maximum-likelihood estimates.
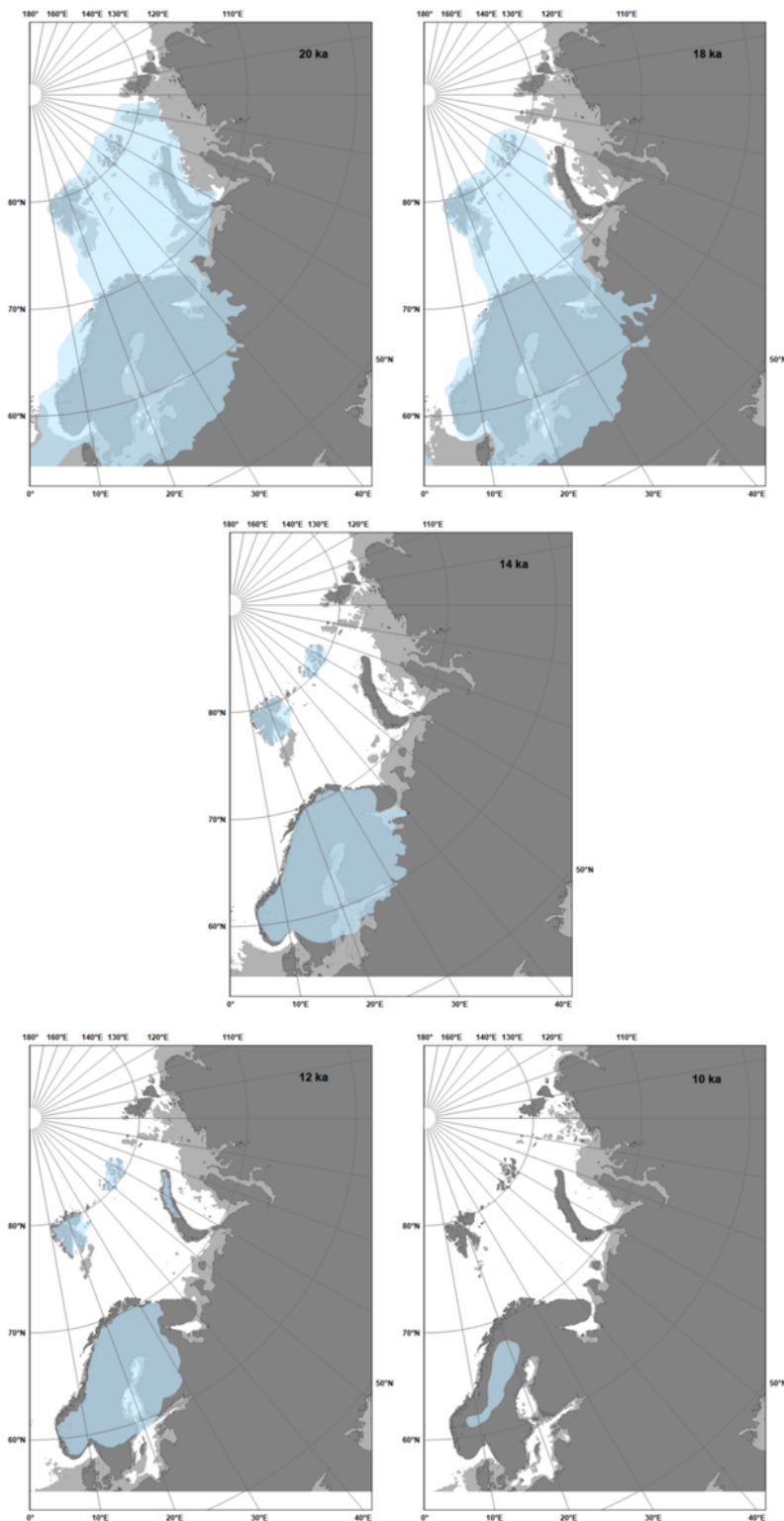

Figure 3

Present land extent (dark grey) and estimated sea level (light grey) overlaid by estimated ice limits (blue) for five different times in the past. The map was constructed in ArcView (ESRI 2011) from ETOPO1 1 arc

minute data (Amante and Eakins 2009). The ice sheet extents are from Hughes et al. 2016. No proglacial lakes are shown, but see Mangerud et al. (2004). Sea levels at each time in were according to Lambeck et al. (2014).

Supplementary Files

This is a list of supplementary files associated with this preprint. Click to download.

- OnlineResources1and2.docx
- OnlineResource3Table1.xlsx
- Table1.docx
- Table2.docx